

# Biological acellular pericardial mesh regulated tissue integration and remodeling in a rat model of breast prosthetic implantation

Roberta Bernardini<sup>1†</sup> | Dimitrios Varvaras<sup>2†</sup> | Federico D'Amico<sup>3†</sup> |  
Alessandra Bielli<sup>3†</sup> | Maria Giovanna Scioli<sup>3</sup> | Filadelfo Coniglione<sup>4,5</sup> | Piero Rossi<sup>2</sup> |  
Oreste C. Buonomo<sup>2</sup> | Giuseppe Petrella<sup>2</sup> | Maurizio Mattei<sup>1,6‡</sup> | Augusto Orlandi<sup>3,5‡</sup>

<sup>1</sup>Centro Servizi Interdipartimentale—STA, University of Rome "Tor Vergata", Rome, Italy

<sup>2</sup>Department of Experimental Medicine and Surgery, University of Rome "Tor Vergata", Rome, Italy

<sup>3</sup>Anatomic Pathology, Department of Biomedicine and Prevention, University of Rome "Tor Vergata", Rome, Italy

<sup>4</sup>Department of Clinical Science and Translational Medicine, University of Rome "Tor Vergata", Rome, Italy

<sup>5</sup>Department of Biomedical Sciences, Catholic University Our Lady of Good Counsel, Tirana, Albania

<sup>6</sup>Department of Biology, University of Rome "Tor Vergata", Italy

## Correspondence

Augusto Orlandi, Institute of Anatomic Pathology, Department of Biomedicine and Prevention, University of Rome "Tor Vergata", Via Montpellier 1, 00133 Rome, Italy.  
Email: orlandi@uniroma2.it

## Funding Information

Assut Europe S.p.A

## Abstract

The use of biological meshes has proven beneficial in surgical restriction and periprosthetic capsular contracture following breast prosthetic-reconstruction. Three different types (smooth, texturized, and polyurethane) of silicone round mini prostheses were implanted under rat skin with or without two different bovine acellular pericardial biological meshes (APMs, BioRipar, and Tutomesh). One hundred eighty-six female rats were divided into 12 groups, sacrificed after 3, 6, and 24 weeks and tissue samples investigated by histology and immunohistochemistry. Implantation of both APMs, with or without prostheses, reduced capsular  $\alpha$ -SMA expression and CD3<sup>+</sup> inflammatory cell infiltration, increasing capillary density and cell proliferation, with some differences. In particular, Tutomesh was associated with higher peri-APM CD3<sup>+</sup> inflammation, prosthetic capsular dermal  $\alpha$ -SMA expression and less CD31<sup>+</sup> vessels and cell proliferation compared with BioRipar. None differences were observed in tissue integration and remodeling following the APM + prostheses implantation; the different prostheses did not influence tissue remodeling. The aim of our study was to investigate if/how the use of different APMs, with peculiar intrinsic characteristics, may influence tissue integration. The structure of APMs critically influenced tissue remodeling after implantation. Further studies are needed to develop new APMs able to optimize tissue integration and neoangiogenesis minimizing periprosthetic inflammation and fibrosis.

## KEYWORDS

animal model, breast reconstruction, capsular contracture, pericardium dermal biological mesh, silicone implants

## 1 | INTRODUCTION

Breast cancer is the second most common cancer in the world and the most common cancer among women with estimated 1.67 million

new cases diagnosed every years (Cancer WHOIAfRoG, 2015). Breast cancer was also the most common cancer amongst Italian woman population, with 51,000 new diagnoses (AIOM, 2018; Epidemiologia e Prevenzione, 2013). Advances in early detection, identification of subjects at the high risk of developing cancer in familial-hereditary status, oncological and breast studies are progressively stretching out their limits over the prolongation of patients overall survival (OS) and the

<sup>†</sup>These authors contributed equally as First Author.

<sup>‡</sup>These authors contributed equally as Last Author.

disease-free survival (DFS) and gradually moving their efforts at the quality of life concept (Ng et al., 2008). Approximately 35–40% of women diagnosed with breast cancer undergo a surgical mastectomy and about a third of them undergo to breast reconstruction (BR) after mastectomy (DellaCroce & Wolfe, 2013).

Breast reconstruction represents an essential element of the therapeutic procedure in women with breast cancer treated with mastectomy, since it reduces negative effects on body image deriving from the destructive surgical procedures (Kocan & Gursoy, 2016). Consequently, breast reconstruction is requested by an increasing number of patients in order to maintain femininity and a good quality of life without affecting the prognosis. Breast reconstruction generally consists of two stages: restoration of the breast mound and reconstruction of the nipple-areola complex (Somogyi, Ziolkowski, Osman, Ginty, & Brown, 2018). Reconstruction of the breast mound itself can be performed with the use of either implants or autogenous tissues (Gardani et al., 2017). The choice of the technique depends on many factors, including breast size and shape, the location and type of cancer, the availability of tissues around the breast and at other sites, the patient's age and potential clinical risk factors, including the type of adjuvant therapy (Bodai & Tusso, 2015). The final decision is often made in accordance with the patient's preference. Prosthetic breast reconstruction has the advantages of shorter procedure time, hospital stay and recovery as well as lower costs (Racano et al., 2002) and does not need for an additional patient's autologous tissue donor site (Roostaeian et al., 2012). The different options for prosthetic-based breast reconstruction include a two-stage reconstruction with a tissue expander followed by a permanent prosthesis and most of the time with intervening adjuvant therapy, a process named delayed breast reconstruction. Alternatively, at the time of the mastectomy, an immediate single-stage reconstruction with prosthesis is provided, as well as a reconstruction with the combination of prosthesis and autologous tissue transplantation (Bertozi, Pesce, Santi, & Raposio, 2017). Immediate breast reconstruction has steadily increased since 2005 (Sabino et al., 2016) and allows to obtain an immediate aesthetic result improving the patient's compliance by restoring mammary volume and shape (Chang, Hargreaves, Segara, & Moisisidis, 2013). Unfortunately, immediate breast reconstruction is appropriate only for a small number of patients who has not big or ptotic breast, and has a good quality of skin and muscles for immediate prosthesis placement. The disadvantage of immediate-breast reconstruction is that aesthetic outcomes does not tend to be as good as delayed-breast reconstruction and, in many cases, a second surgical procedure is required (Gardani et al., 2017). Breast prostheses can be of two types, based on saline or silicone gel content, and have an external solid silicone shell that can be smooth, textured or polyurethane (Maxwell & Gabriel, 2017). The chronic inflammatory response due to the surgical installed foreign object-breast implant induces a reactive myofibroblast-driven fibrous encapsulation, with tightly collagen fibers accumulation (Silva et al., 2011). The development of a fibrous capsule around prosthesis and its contraction is a critical point, and may result in a stiffer and thicker capsule (DiEgidio et al., 2014). The latter determines pain, soft tissue irritation and leads, from the aesthetic point of view, an undesirable breast appearance

(Administration FaD, 2011). Capsular contracture is the most common complication associated with prosthetic breast reconstruction following mastectomy for cancer, with a frequency of 21.8 and 34% at 5 years, respectively (Caffee, 1986) and it has a multifactorial origin (Schmitz, Bertram, Kneser, Keller, & Horch, 2013; Seyhan et al., 2011). In the recent years different surface materials and interfaces between silicone prostheses and the implant site have been projected and used in order to avoid the direct contact between silicone and host tissue and consequently to reduce the extent of capsular contracture (Headon, Kasem, & Mokbel, 2015). Biological matrices have been demonstrated to be particularly suitable to this aim (Schmitz et al., 2013). Advantages to use a acellular bovine pericardium-derived collagen matrix membrane (APM) as a biological mesh include the capability to facilitate the surgical procedures of immediate-breast reconstruction, the improvement of the definition of the inframammary and lateral mammary fold and the decreased rate of capsular contracture (Gubitosi et al., 2014). Nevertheless, data concerning differences in tissue remodeling according to the type of biological mesh on surface prostheses have been not deeply investigated. To this aim, we analyzed tissue remodeling occurring after implantation of two different bovine pericardium-derived biological meshes and three different types (smooth, texturized and polyurethane) of mini-silicone round prosthesis in a rat model. Our data indicated that tissue remodeling can vary mostly according to the employed APM and suggest further studies to develop a new biological mesh capable to further reduce prostheses-induced adverse effects following breast reconstruction.

## 2 | MATERIALS AND METHODS

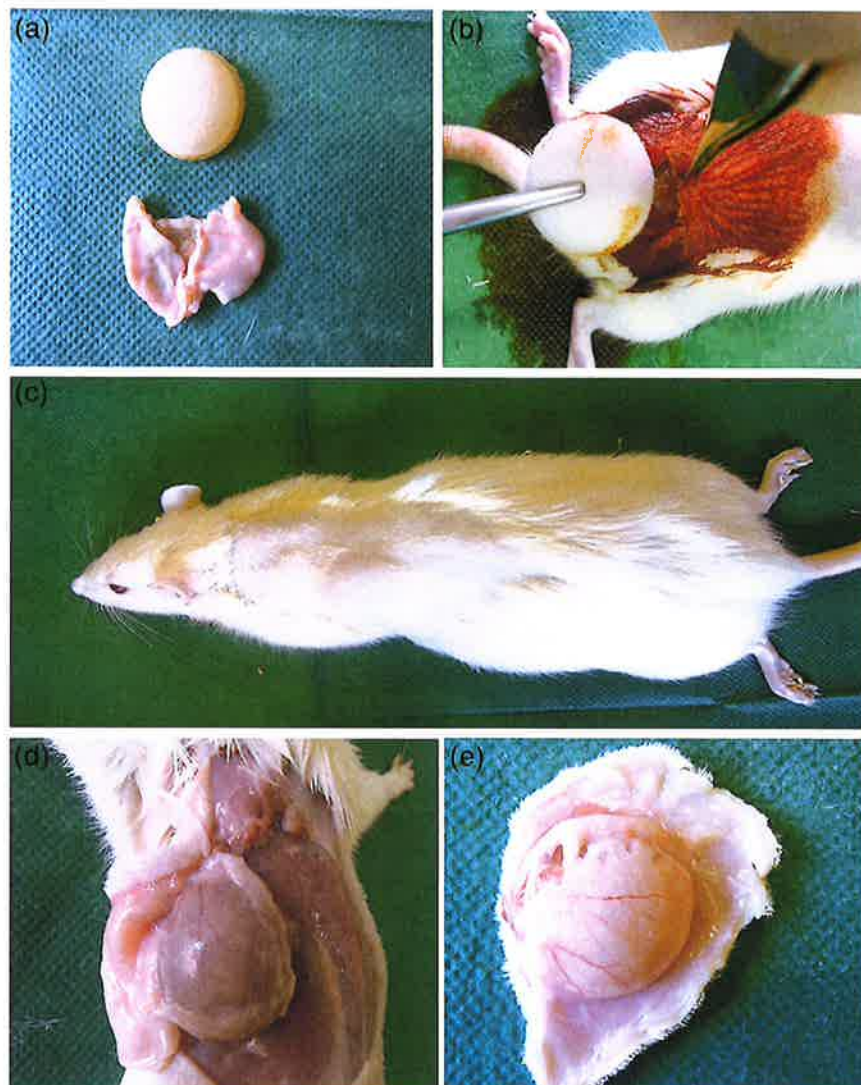
### 2.1 | Biological meshes and implants

For this study, two different APMs were used: BioRipar (ASSUT-EUROPE, Rome, Italy), and Tutomesh® (Tutogen Medical GmbH, Neunkirchen am Brand, Germany) (Figure 1). APMs decellularization method was previously described (Bielli et al., 2018). One hundred-thirty five silicone gel-filled miniprotheses were employed (SILIMED-TM, Company, São Paulo, Brazil). The prostheses were of three different types with round base and equal volume (2 cm<sup>3</sup>): smooth (S) (diameter 2.0 × thickness 0.85 cm), textured (T) (2.2 × 0.85 cm) and polyurethane (P) (2.3 × 0.85 cm).

### 2.2 | Mechanical characterization

We previously compared mechanical properties of BioRipar and Tutomesh® by using two mechanical tests, namely uniaxial tensile test and burst test (Bielli et al., 2018). We tested APM stiffness by using a load applied in-plane (tensile stiffness) and a load applied perpendicular to the mesh (distension). Tensile strength (MPa, N/mm<sup>2</sup>), in wet and dry conditions, was than calculated (Supplemental Figure I). Mechanical tests were carried out in an ISO 17025 Accredited Laboratory (Brachi Testing Services Srl, Prato Italy) (Bielli et al., 2018).

**FIGURE 1** Acellular pericardial biomesh implantation and gross examination. (a) Example of APM and prostheses used for surgical implantation. (b) Surgical procedure in rat. (c) Implantation of APM + prostheses in rat. (d,e) Macroscopic examination of APM + prostheses integration with surrounding tissue after 24 weeks



## 2.3 | Transmission electron microscopy

Structural and morphological integrity of APMs were investigated by transmission electron microscopy (TEM), in fixed Karnovsky small tissue samples as reported (Bielli et al., 2018; Orlandi, Francesconi, Cocchia, Corsini, & Spagnoli, 2001). Ultrathin sections were counterstained and photographed by a Hitachi 7100FA transmission electron microscope as reported.

## 2.4 | Animals

The study enrolled 177 adult female Wistar rats, weighing 180–220 g (Harlan Laboratories, IN). Animals were housed under standard laboratory conditions: light/dark cycles (12/12 hr), ambient temperature  $20 \pm 2^\circ\text{C}$ , 55% relative air humidity and food (Mucedola RF18) and water ad libitum. All experiments were approved by the Institutional Animal Care and Use Committee (IACUC) and carried out according to the

Italian and European rules (D.L.vo 116/92; C.E. 609/86; European Directive 2010/63/EU). A veterinary surgeon was present during the surgical procedure and blood sample collection. Animal handling, before and after experiment, was carried out only by trained personnel. After surgery, gross visual observations were made daily for general condition (appearance, attitude, appetite, hydration), body weight and food consumption. After 14 days the incision heal was complete and staples removed. Two animals from the control group and five animals from each other group were sacrificed in saturated  $\text{CO}_2$  chamber at the following time: 3, 6, and 24 weeks (Supplemental Table I).

## 2.5 | Experimental design and surgical procedure

Thirty rats randomized in two groups were subjected to the implantation of two different APMs, in the dorsum. Forty-five rats were randomized in three groups and subjected to the implantation of three

different silicone gel-filled miniprotheses. Other 90 rats were randomized in six groups and underwent to the implantation of different silicone gel filled miniprotheses overlaid with the two different APMs (Figure 1). Experimental groups are described in Supplemental Table I. All surgical procedures were performed under general anesthesia by intra-abdominal injection of tiletamine/zolazepam (50 mg/kg Zoletil 100, Virbac, Italy) associated to xylazine (15 mg/kg Rompun, Bayer, Italy). Under anesthesia, each animal was placed in the prone position. After epilation on the dorsum, from tail up to cervical region, the skin was disinfected with a povidone iodine solution. The surgical sites were located 3 cm above the hind limbs in the lumbar region. After making a 4 cm of transverse skin incision, a tunnel was created. Through the incision, meshes, prostheses, meshes plus prostheses were placed in a pocket between the shoulder blades.

The subcutaneous tissue and skin were closed by skin staplers (Appose™-ingle Use Skin Stapler-COVIDIEN PRODUCTS by Medtronic, Regular Staple-width/crow 4.8 mm and leg length 3.4 mm).

## 2.6 | Follow-up and macroscopic assessment

The macroscopic appearance of wounds and pocket implants was carefully inspected for dislocation or extrusion of the prostheses, as well for abscess, hematoma, and seroma or wound dehiscence. At all-time points, macroscopic evaluations showed no local adverse effects for each groups and no biologically significant differences in the post-operative course was found. No animals were lost due to surgery and most skin lesions were macroscopically filled with repair tissue at 2 weeks after operation. No findings of postoperative infection, hematoma, seroma, implant infection or implant extrusion or lost were observed.

## 2.7 | Blood collection

To evaluate blood reaction to the different meshes and implants, retro-orbital blood collection after 3 and 24 weeks, was performed. Fifty microliters of whole blood were collected in K2EDTA microtainers (Boston, Dickinson and Company, USA) and analyzed using the automated cell counter "Drew3" (BPC BioSed, Italy). For cytomorphological examination, each peripheral blood smears were prepared using the Diff-Quick staining (Dade SpA, Italy) and analyzed under optical microscopy. For serum protein electrophoresis, blood samples were collected in SST microtainers (Serum Separator Tube; Boston, Dickinson and Company), centrifuged in a microcentrifuge (5415R model; Eppendorf, Italy) at 13,000 rpm for 7 min to separate the serum, and used with cellulose polyacrylate electrophoresis strips for the automatic analyzer Simply Phor (BPC BioSed, Italy).

## 2.8 | Evaluation of hypersensitivity reaction

Twenty weeks after the implantation, three rats from each group were challenged intradermally, in right-hind foot pad, with 50  $\mu$ L of mesh extract after local anesthesia (EMLA, AstraZeneca S.p.A., Italy). Mesh extract was prepared following the international procedure (ISO

10993-12:2007). Thirty days before the test, three rats were inoculated by subcutaneous route with 20  $\mu$ L of PPD (1 mL ampoule of Purified Protein Derivative; Bulbio, Bulgaria) and successively injected with a challenge dose of the same antigen (5  $\mu$ L in 45  $\mu$ L of PBS) into the right-hind footpad as positive control. The contralateral paw received saline alone injected with syringe microfine 30G (Becton, Dickinson and Company, Italy). The thickness of foot pad was measured at 24, 48 and 72 hr after challenge using fine micrometer (1/100 cm sensitivity) (H. Kunkel, Offenbach, Germany). The difference in the thickness of hind paw was used as a measure of delayed type hypersensitivity reaction, subtracting the thickness of the time zero from the values obtained at 24, 48, and 72 hr after challenge.

## 2.9 | Microscopic examination and histological analysis

APMs and silicone prostheses were removed "en-bloc" including over-head skin. Samples, with at least 2 cm surrounding tissue, were trimmed and fixed in neutral buffered formaldehyde for 48 hr and the embedded in paraffin for histological and immunohistochemical analysis (Orlandi, Francesconi, Marcellini, Ferlosio, & Spagnoli, 2004). In particular, Hematoxylin&Eosin staining was performed to measure the perimesh space (the distance between the mesh and the point of origin of its implant expanding over the time). Slides were captured under a light microscope (Eclipse E600; Nikon, Tokyo, Japan) at 2x magnification and perimesh space analyzed by the ImageJ 1.50i software. Moreover, Masson's trichrome-staining (Orlandi et al., 2005) was performed to highlight the intrinsic features of the two biological meshes; in particular to assess the collagen and elastic composition of the meshes and possible changes over the time after implantation. Masson's trichrome-staining intensity was arbitrarily scored on a scale of four grades: 0 = negative, 1 = weak positivity, 2 = moderate positivity, 3 = strong positivity.

## 2.10 | Immunohistochemistry

Immunohistochemistry was performed using mouse monoclonal anti- $\alpha$ -SMA, anti-Ki67, anti-CD31 and anti-CD3 antibody (DakoCytomation, Denmark). Normal rat tissue was used as control. The percentage of Ki67<sup>+</sup> cells and the number of CD31<sup>+</sup> vessels/mm<sup>2</sup> were calculated according to histomorphometric criteria (Scioli et al., 2014; Stasi, 2010);  $\alpha$ -SMA staining intensity was arbitrarily scored using a scale of four grades: 0 = negative, 1 = weak positivity, 2 = moderate positivity, 3 = strong positivity. Values were determined in at least 10 randomly selected fields at 400x magnification (Stasi, 2010). Blinded microscopic measurements were performed by two independent researchers, with an interobserver reproducibility >95%.

## 2.11 | Statistical analysis

Data were expressed as mean  $\pm$  SD or SEM. For graph and statistical analysis, the GraphPad Prism 5 (GraphPad Software) computer program was used. The statistical analysis was performed by using one-way ANOVA.  $p \leq .05$  was considered as a significant difference.

### 3 | RESULTS

#### 3.1 | Mechanical and structural properties

The previous evaluation of mechanical properties showed that BioRipar was able to resist at higher tensile stress than Tutomesh APM (Bielli et al., 2018). Also, in the bursting strength test, BioRipar reported the best result, as reported in our previous study (Bielli et al., 2018). Ultrastructural analysis by TEM showed a well-preserved extracellular matrix structure, normal collagen fibers with a regular distribution and transverse banding in both APMs (Supplemental Figure II). The analyses revealed no significant differences between the two APMs, in both wet and dry condition.

#### 3.2 | Gross examination

At the time established by the experimental protocol, after objective examination, sacrifice of the animals was performed. No infection or clinically relevant complication were observed. In the control groups, where only the surgical procedure was performed, tissue was normal to palpation with no postoperative complications. After 24 weeks from implantation of APMs alone, rats' neovascularization and a good integration into the surrounding fibrous connective tissue were documented. A thin, well-vascularized and nonadherent capsule was found around the implant and prostheses in all groups already starting from 3 weeks. Groups with prostheses covered by meshes showed on the external side of the implant a thin layer of vascularized tissue already starting from 3 weeks (Figure 1d,e). Delayed-type hypersensitivity response remained unchanged 24, 48, and 72 hr after BioRipar and Tutomesh APM implantation and similar to the negative controls (Supplemental Figure III).

#### 3.3 | Hematological parameters

To determine whether APM and prosthesis implant had side effects, hematological and serum parameters were analyzed after 6 and 24 weeks. Rats implanted with APM + prosthesis or prosthesis/APM alone showed slight differences of some hematological parameters compared with control. Although some variations (i.e., for Mean Corpuscular Hemoglobin Concentration, Red Cell Distribution Width, Mean Platelet Volume and Platelet Count were significant ( $p < .05$ ), those values fell within the reported reference values of Wistar rats strain (Harlan Laboratories) obtained under the same conditions of housing, sex and age (see Supplemental Figure IV and Supplemental Table II-IX).

#### 3.4 | APM-dermal tissue integration and angiogenesis

To evaluate tissue integration, we performed microscopic and immunohistochemical examination of implanted APM-dermal tissue complex. Morphometric analysis (Figure 2a) revealed no significant difference between BioRipar and Tutomesh APM groups at 3, 6, and 24 weeks. Also fibrous tissue thickness was similar comparing the two APMs

(Supplemental Figure V). Masson's trichrome staining evidenced a different staining pattern between APMs, likely due to their intrinsic characteristics (Figure 2b). Moreover, at 24 weeks after implantation, both APMs showed loose connective tissue rather than fibrotic one.

Immunohistochemistry for the endothelial marker CD31 revealed that implantation of both APMs associated to a significant progressive increase of peri-APM neoangiogenesis, comparing 3 and 24-week data ( $p < .05$ ). Nonetheless, we documented a higher number of CD31<sup>+</sup> small vessels in the implanted BioRipar APM-dermal tissue complex compared with Tutomesh one at 3, 6, and 24 weeks ( $p < .01$ , Figure 3a,c). APM-induced neoangiogenesis associated with an increased cell proliferation (Ki67 immunoreactivity), greater in BioRipar than Tutomesh APM after 3 and 6 weeks from implantation ( $p < .001$ , Figure 3b,d). However, after 24 weeks, BioRipar values decreased becoming similar to Tutomesh ones. To assess the contribution of myofibroblasts to the APM-induced fibrosis encapsulation, we evaluated  $\alpha$ -SMA expression (Yamashita et al., 2012) around implanted APMs. As shown in Figure 4,  $\alpha$ -SMA immunoreactivity was higher in Tutomesh compared with BioRipar group at 3 and 6 weeks after implantation ( $p < .05$ , Figure 4a,c). After 24 weeks,  $\alpha$ -SMA immunoreactivity decreased in Tutomesh becoming similar to BioRipar group (Figure 4a,c).

#### 3.5 | APM-dermal tissue integration and inflammation

Inflammatory T-cell infiltrate, peri-APM and intra-APM, was analyzed by CD3 immunostaining (Figure 4b,d and Supplemental Figure IV). A greater number of peri-APM CD3<sup>+</sup> cells was observed at 3 weeks after implantation in Tutomesh compared with BioRipar group ( $p < .001$ ). After 24 weeks, CD3<sup>+</sup> values were reduced in Tutomesh and become similar to BioRipar group ( $p < .05$ ). No difference in intra-APM T-cell inflammatory infiltrate was observed comparing APMs groups (change in Supplemental Figure VI). CD3<sup>+</sup> values, in intra- and peri-APM sites, remained high in both APMs also after 24 weeks from implantation, suggesting a chronic T-cell-mediated inflammation.

#### 3.6 | Tissue integration of APMs covering silicone prostheses

We also investigated APMs-dermal tissue integration after a combined implantation with silicone prostheses. Three weeks after implantation, no difference in the number of CD31<sup>+</sup> vessels was observed within BioRipar+prostheses group (Figure 5a,c), but values were greater than those of corresponding Tutomesh+prostheses groups ( $p < .05$ ,  $p < .01$ , and  $p < .01$ , respectively). Within Tutomesh group, the combination with smooth prostheses showed a higher number of CD31<sup>+</sup> vessels compared with Polyurethane ( $p < .05$ , Figure 5b,c). Similarly, at 6 and 24 weeks after implantation, although with some differences, CD31<sup>+</sup> vessels were more in BioRipar+prostheses compared with Tutomesh+prostheses groups ( $p < .01$ ,  $p < .01$  and  $p < .01$ , respectively). As reported in Figure 6, intra-APM Ki67<sup>+</sup> cells were more in BioRipar+prostheses compared with Tutomesh+prostheses groups, in particular after 3 and 6 weeks ( $p < .01$ ,  $p < .01$ , and  $p < .01$ , respectively Figure 6a,b). After



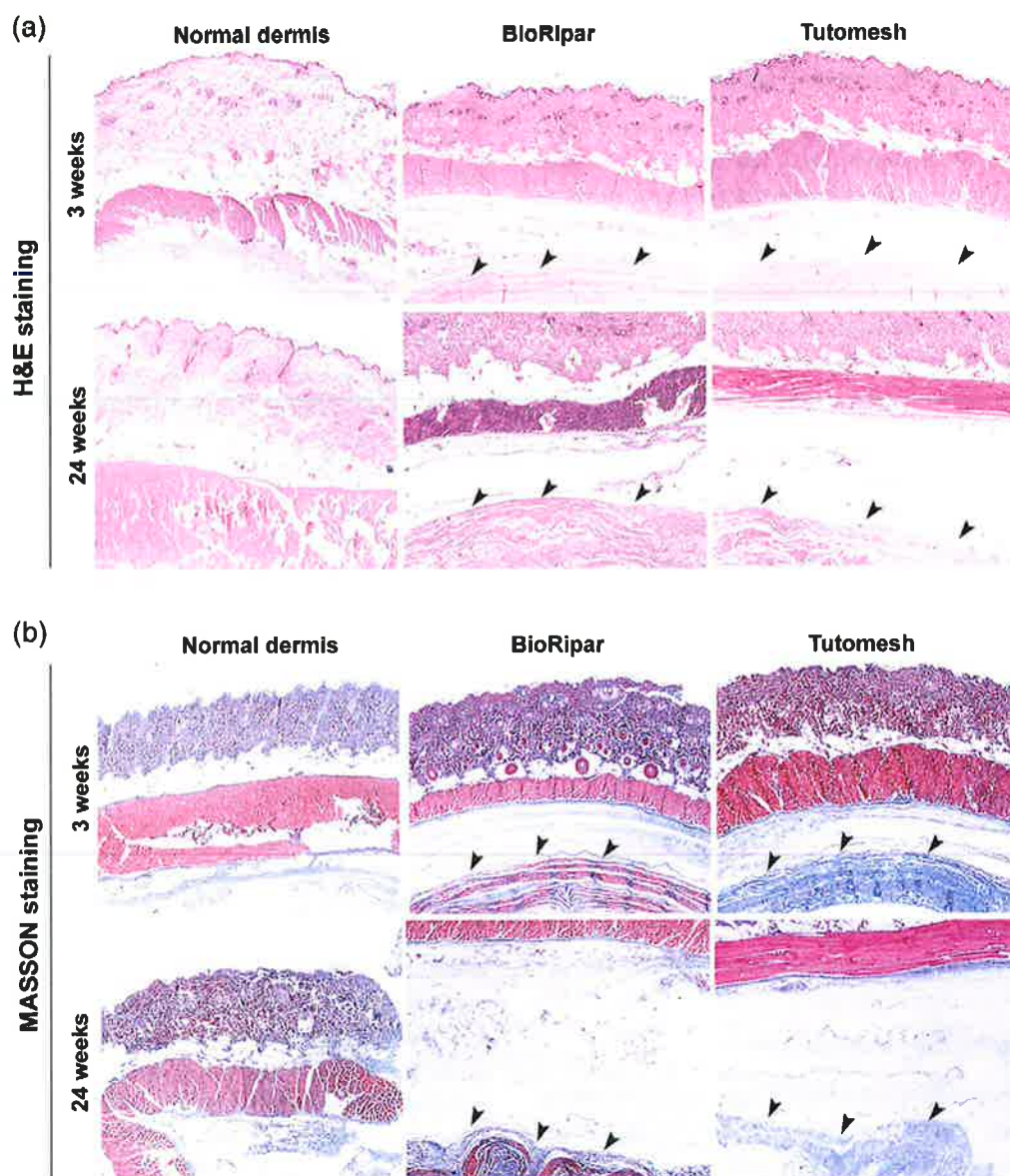


**FIGURE 2** Microscopic evaluation and histological analysis after BioRipar and Tutomesh APMs implantation. (a) Representative microscopic images of Haematoxylin&Eosin (H&E)-stained tissue sections at 3 and 24 weeks after implantation compared with normal dermis of control. (b) Representative microscopic images of Masson's trichrome-stained tissue sections 3 and 24 weeks after APM implantation compared with normal dermis of control s. Arrowheads indicate APMs

6 weeks, BioRipar+Smooth still showed higher cell proliferation than BioRipar-Polyurethane prostheses ( $p < .05$ ). Instead, Tutomesh+Textured prostheses showed a higher number of Ki67<sup>+</sup> cells than Tutomesh+Smooth and Tutomesh+Polyurethane prostheses ( $p < .05$  and  $p < .01$ , respectively). Finally, after 24 weeks, no difference between BioRipar and Tutomesh+prostheses groups was found. Nevertheless, BioRipar

+Textured showed a reduced number of Ki67<sup>+</sup> cells compared with BioRipar+Smooth and BioRipar+Polyurethane prostheses ( $p < .01$ ).

As concerning  $\alpha$ -SMA immunoreactivity, marker of myofibroblast activity, Tutomesh+prostheses groups showed higher values compared with BioRipar+prostheses groups after 3 and 6 weeks ( $p < .05$ ,  $p < .05$ , and  $p < .05$ , respectively; Figure 7a,b). In particular, Tutomesh

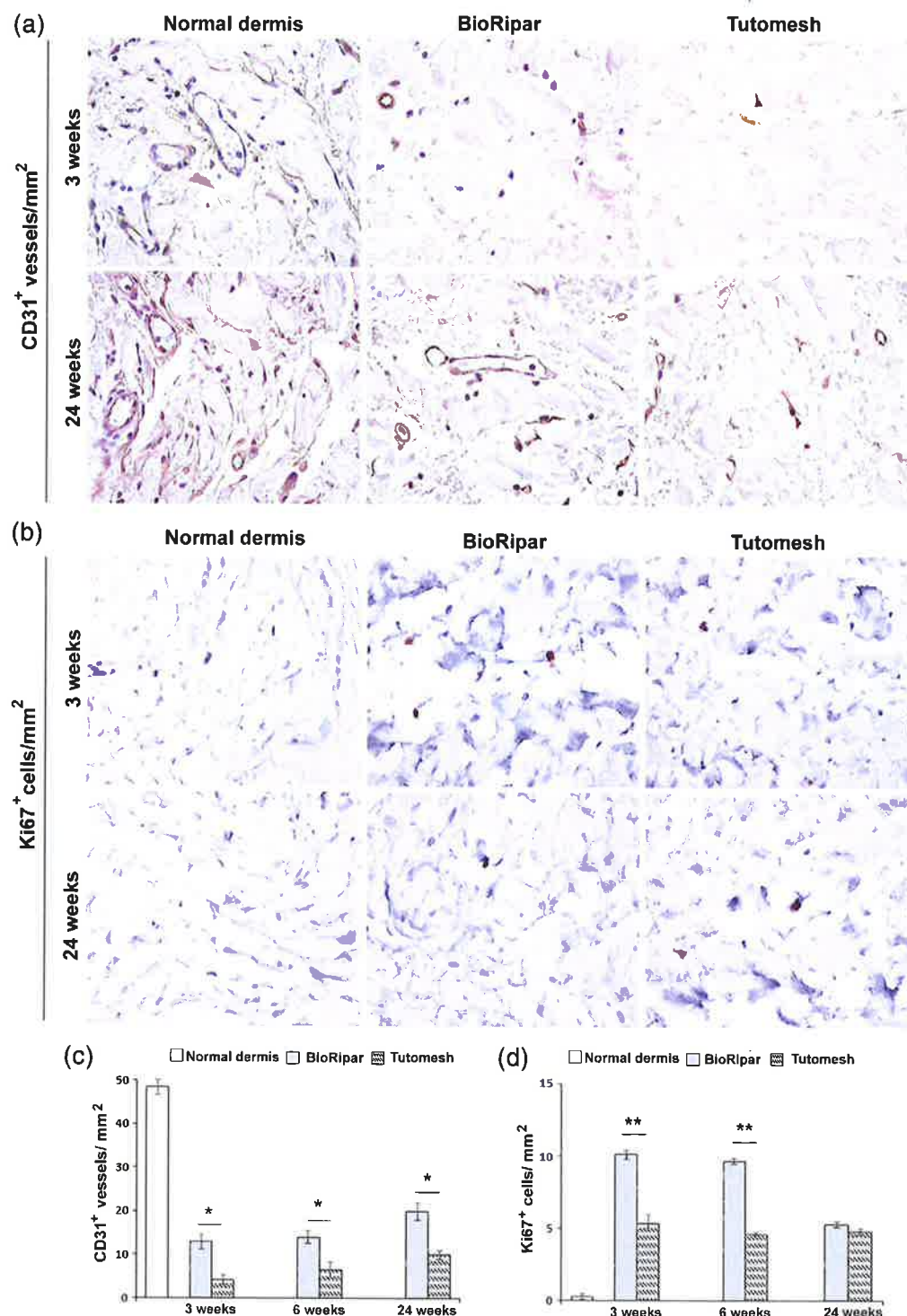


**FIGURE 3** Neangiogenesis and cell proliferation after BioRipar and Tutomesh APMs implantation. (a) Representative microscopic images of tissue samples showing intramesh capillary density CD31<sup>+</sup> vessels per mm<sup>2</sup> 3 and 24 weeks after APM implantation. (b) Representative images of intramesh Ki67<sup>+</sup> cell percentage 3 and 24 weeks after APM implantation. Original magnification  $\times 400$ . (c,d) Bar graphs showing data from immunohistochemical evaluation. t test: \* and \*\*,  $p < .01$  and  $p < .001$ , respectively

+Smooth showed a higher  $\alpha$ -SMA intensity compared with Tutomesh +Textured and Tutomesh+Polyurethane prostheses after 3 weeks ( $p < .05$ ). After 24 weeks, no difference was observed between BioRipar and Tutomesh+prostheses groups. However, BioRipar+Textured

prostheses showed a higher  $\alpha$ -SMA immunoreactivity compared with BioRipar+Polyurethane ( $p < .05$ ).

Evaluation of intra and peri-APM CD3<sup>+</sup> cells in BioRipar and Tutomesh+prostheses groups after 3, 6, and 24 weeks showed the



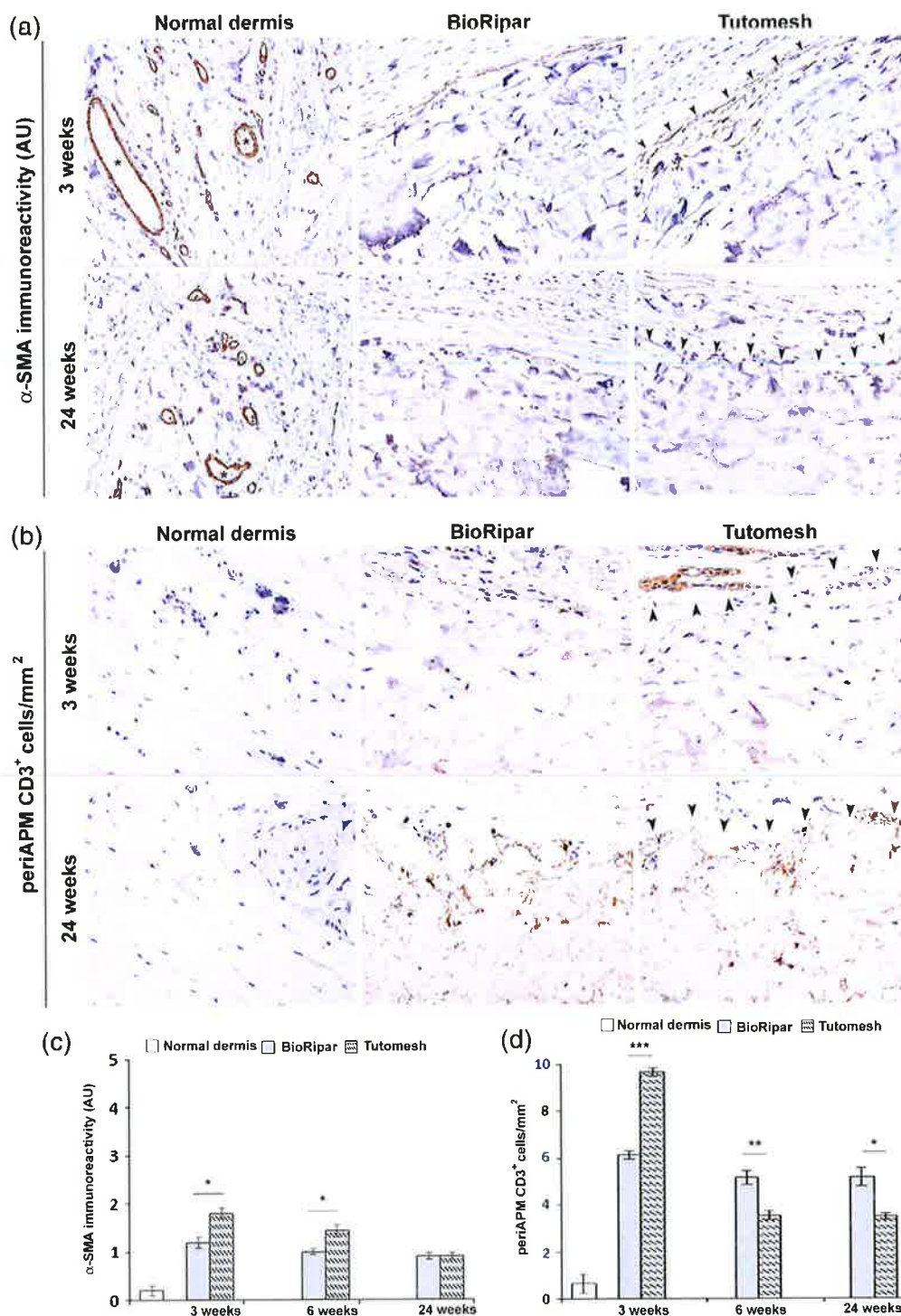


**FIGURE 4** Myofibroblast-driven fibrous encapsulation and inflammatory reaction after implantation of BioRipar and Tutomesh APMs. (a) Representative microscopic images of tissue samples showing  $\alpha$ -SMA<sup>+</sup> myofibroblasts around APM 3 and 24 weeks after implantation. (b). Images of perimesh CD3<sup>+</sup> inflammatory cells 3 and 24 weeks after implantation. Original magnification  $\times 200$ . (c,d) Bar graphs showing data from immunohistochemical evaluation. t test: \*, \*\*, \*\*\*,  $p < .05$ ,  $p < .01$ , and  $p < .001$ , respectively. Asterisks indicate  $\alpha$ -SMA<sup>+</sup> control vessels; arrowheads indicate the interface between dermis and APM implantation. Abbreviation: AU, arbitrary units

same trend observed in the implantation of APM alone (Figure 4d and Supplemental Figure IV). However, some differences were observed among Tutomesh+prostheses groups. In particular, Tutomesh

+Textured prostheses showed a reduced intra-APM CD3<sup>+</sup> infiltrate compared to Tutomesh+Polyurethane prostheses after 3 weeks ( $p < .05$ , Figure 8a,b). Moreover, after 24 weeks, Tutomesh



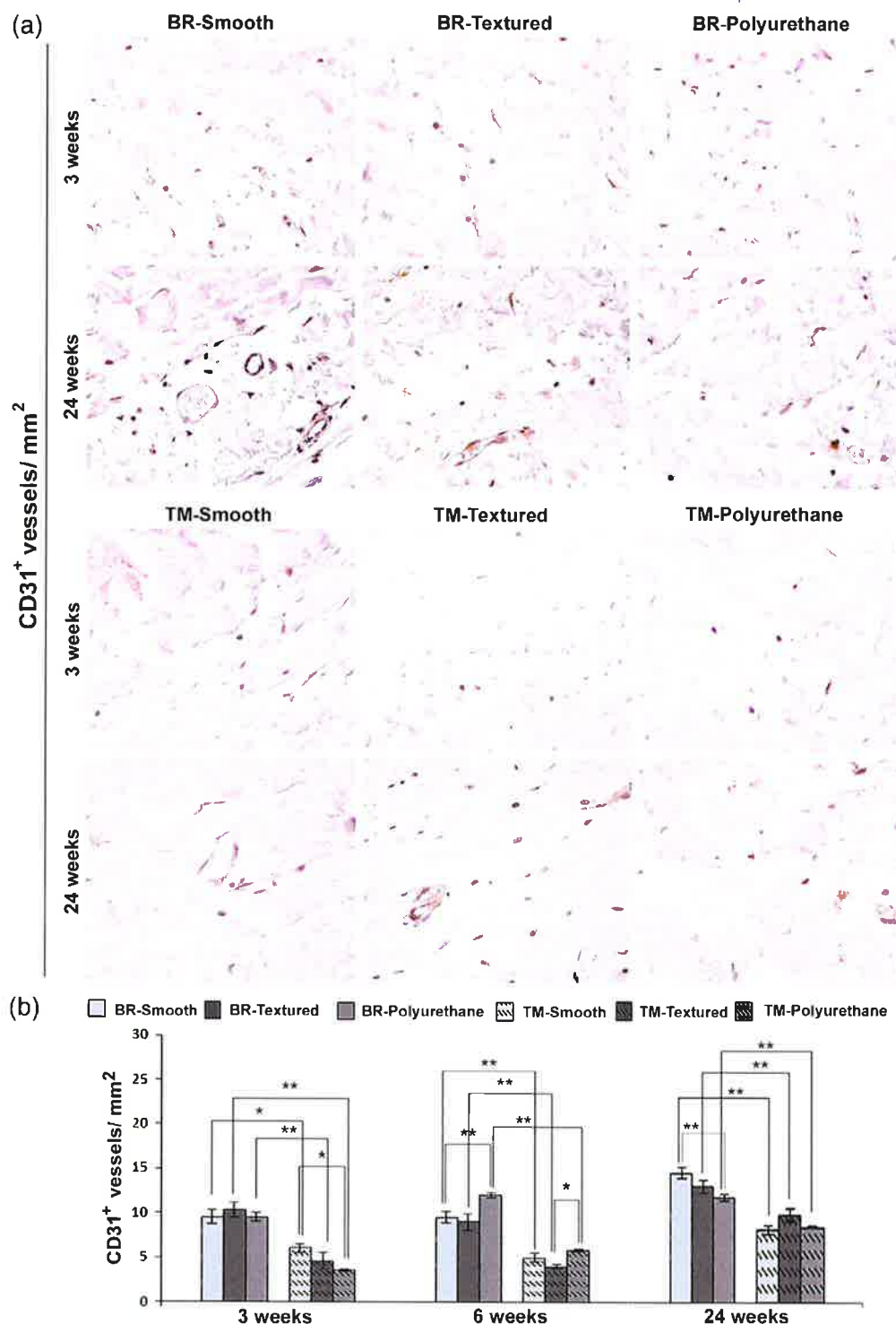


**FIGURE 5** Neangiogenesis after implantation of BioRipar and Tutomesh APMs combined with different silicone prostheses.

(a) Representative microscopic tissue images showing intra-APM capillary density as CD31<sup>+</sup> vessels 3 and 24 weeks after implantation. (b) Bar graphs showing data from immunohistochemical evaluation. Original magnification  $\times 400$ . *t* test: \* and \*\*,  $p < .05$  and  $p < .01$ , respectively.

Abbreviation: BR, BioRipar; TM, Tutomesh

+Polyurethane showed a higher CD3<sup>+</sup> infiltrate compared also with Tutomesh+Smooth ( $p < .05$ ).

Evaluation of peri-APM CD3<sup>+</sup> cells, after 3 weeks, showed a reduction in Tutomesh+Smooth compared with Tutomesh+Textured

prostheses ( $p < .05$ , Figure 8a,b); moreover, significant differences were observed between BioRipar and Tutomesh+prostheses groups ( $p < .01$ ,  $p < .01$ , and  $p < .01$ , respectively, Figure 8a,b). After 6 and 24 weeks, Tutomesh+Polyurethane prostheses showed a lower CD3<sup>+</sup> infiltrate

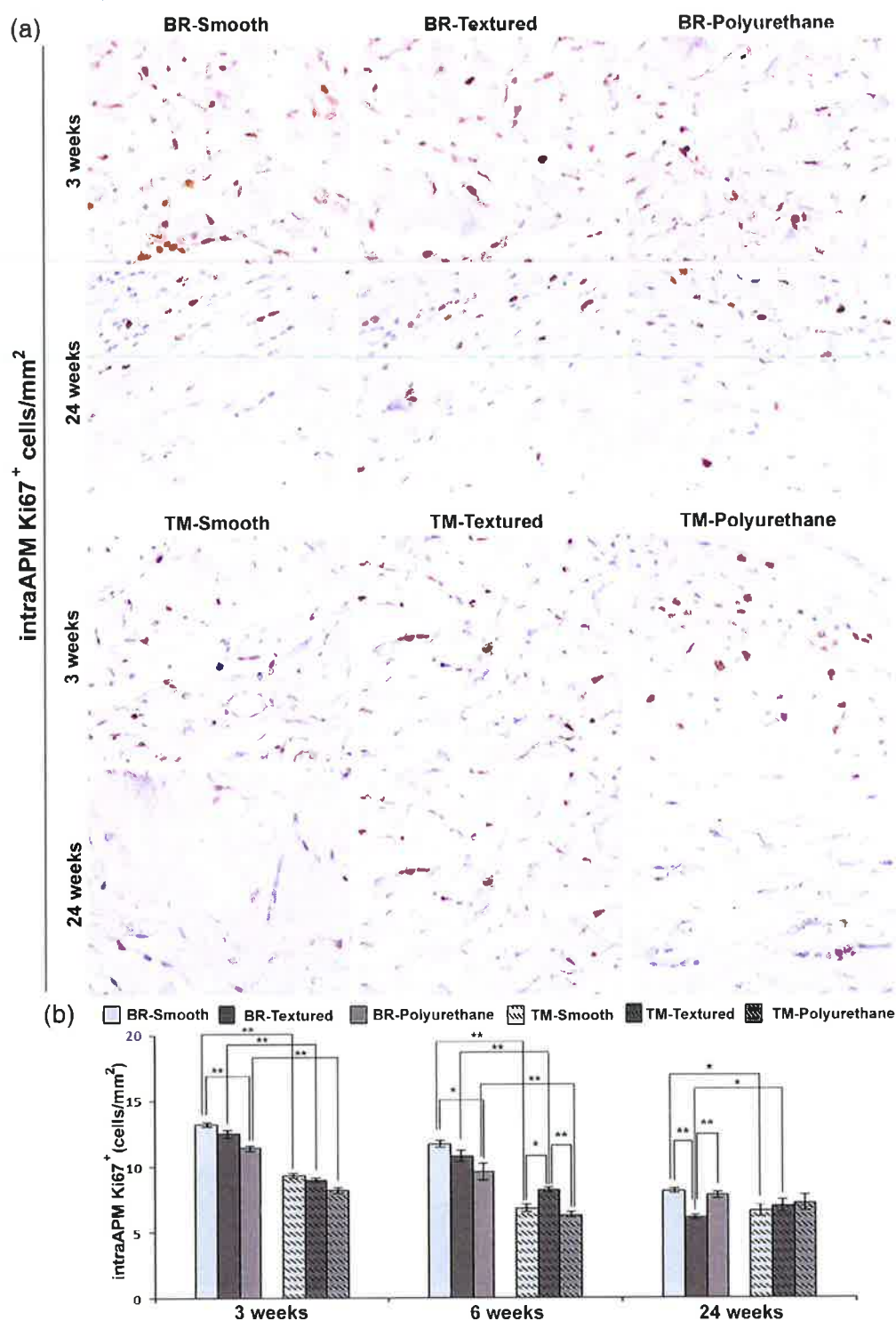


**FIGURE 6** Ki67<sup>+</sup> cell proliferation after implantation of BioRipar and Tutomesh APMs combined with different silicone prostheses.

(a) Microscopies images of dermal samples showing intramesh Ki67<sup>+</sup> cells 3 and 24 weeks after implantation. Original magnification x400. (b) Bar graphs showing data from immunohistochemical evaluation. t test: \* and \*\*,  $p < .05$  and  $p < .01$ , respectively. Abbreviation: BR, BioRipar; TM, Tutomesh

compared with Tutomesh+Textured and Tutomesh+Smooth prostheses groups ( $p < .05$  and  $p < .01$ , respectively). Moreover, after 24 weeks, CD3<sup>+</sup> infiltrate was reduced in BioRipar+Smooth compared with

BioRipar+Textured prostheses ( $p < .05$ , Figure 8a,b), and BioRipar+prostheses group values were significantly greater than those of Tutomesh +prostheses group ( $p < .05$ ,  $p < .01$ , and  $p < .05$ , respectively).

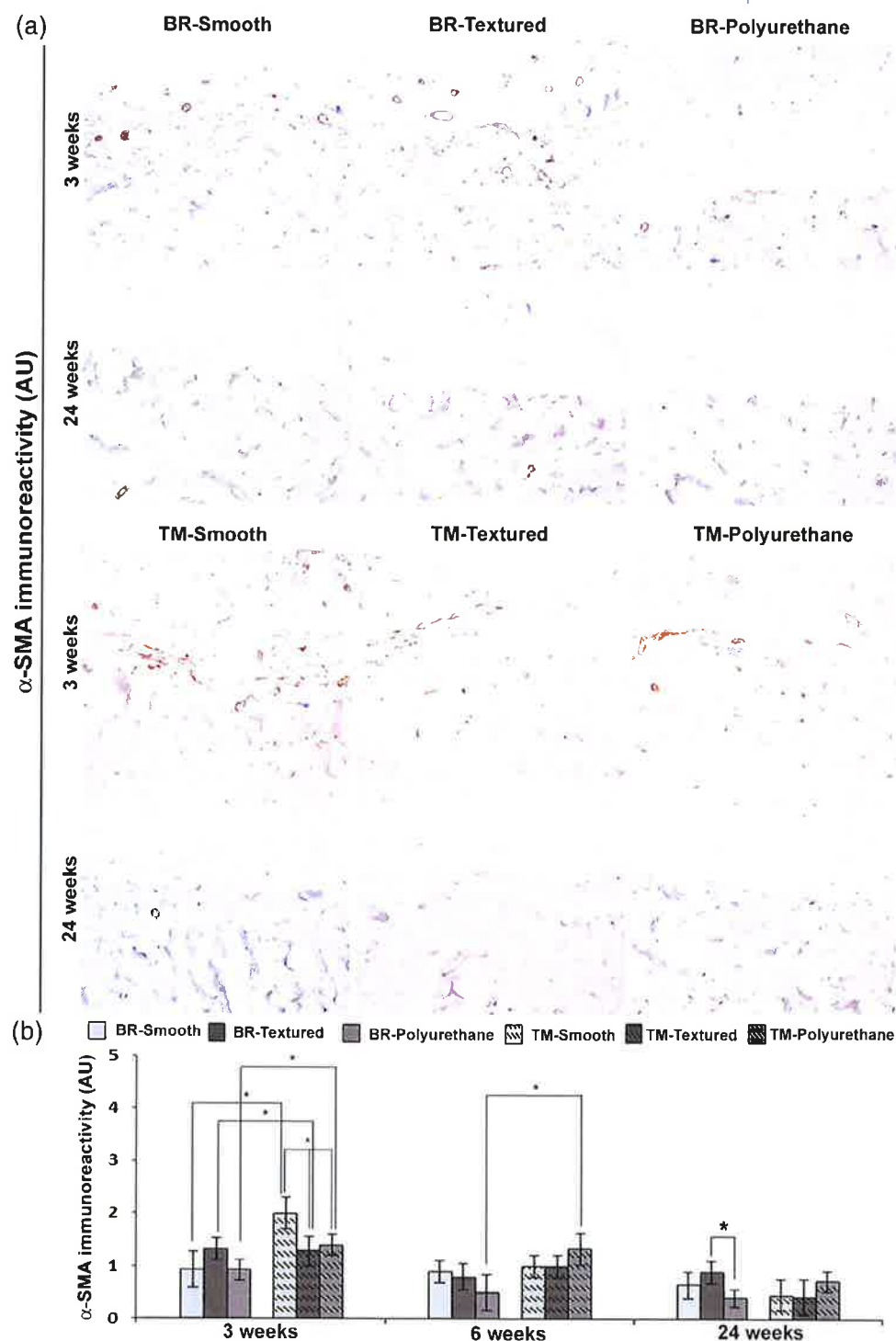


**FIGURE 7** Myofibroblast-driven fibrous encapsulation after implantation of BioRipar and Tutomesh APMs combined with different silicone prostheses. (a) Representative microscopic tissue images showing  $\alpha$ -SMA<sup>+</sup> myofibroblast accumulation around APM 3 and 24 weeks after implantation. Original magnification  $\times 400$ . (b) Bar graphs showing data from immunohistochemical evaluation. t test: \*,  $p < .05$ . Abbreviation: AU, arbitrary units; BR, BioRipar; TM, Tutomesh

## 4 | DISCUSSION

In the present study, we investigated tissue remodeling following APM alone and combined APM and prosthesis implantation in a well-

established rat preclinical model (Mendes, Viterbo, & DeLucca, 2008). The inflammatory response following surgical implantation of prosthesis leads to a myofibroblast-driven fibrotic encapsulation consisting of tightly waver collagen fibers (Darzi et al., 2016). Capsular fibrous

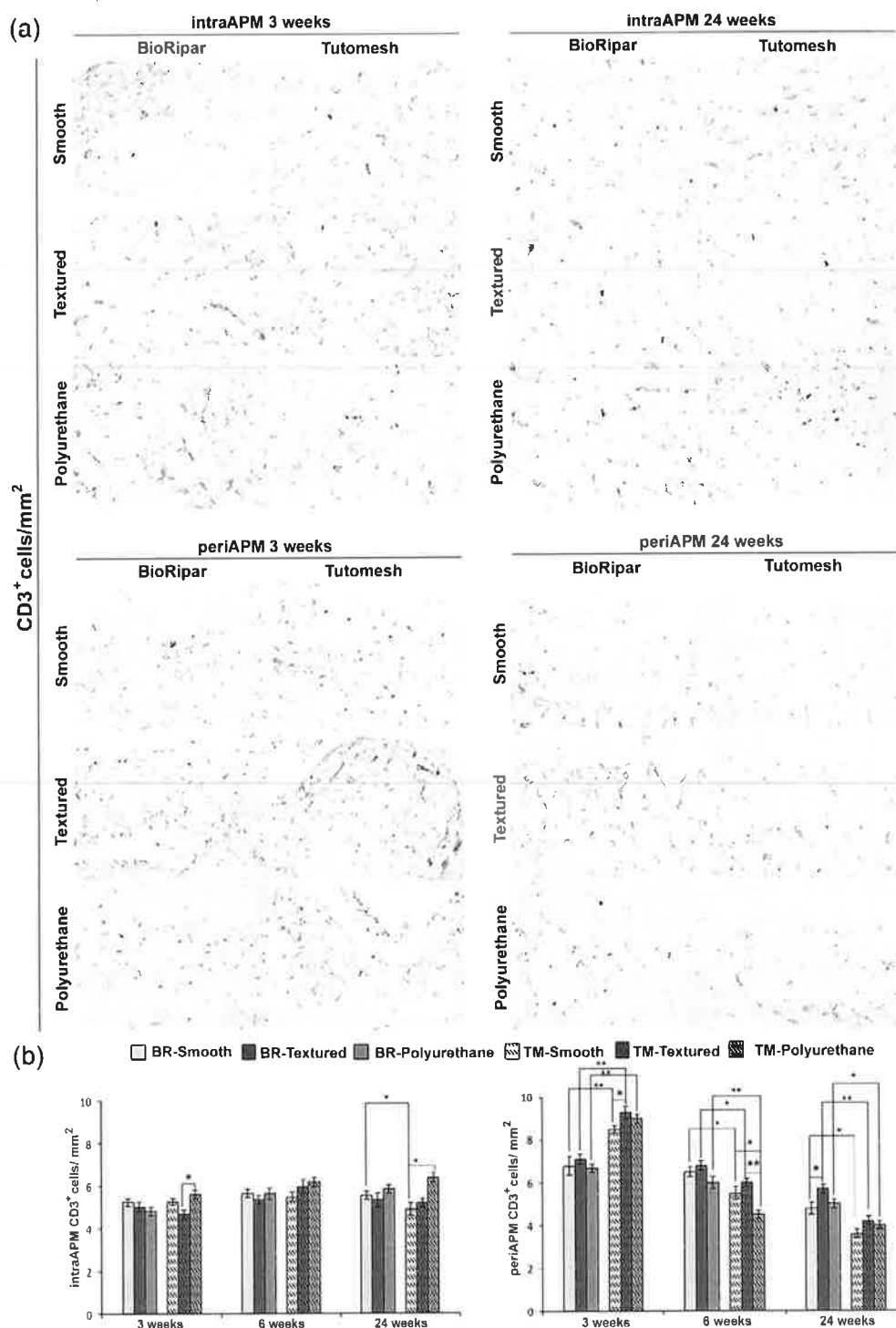


**FIGURE 8** Inflammatory CD3<sup>+</sup> reaction after implantation of BioRipar and Tutomesh APMs combined with different silicone prostheses. (a) Images of intramesh and perimesh CD3<sup>+</sup> inflammatory cells 3 and 24 weeks after implantation. (b) Bar graphs showing data from immunohistochemical evaluation. Original magnification  $\times 200$ . t test: \* and \*\*,  $p < .05$  and  $p < .01$ , respectively. Abbreviation: BR, BioRipar; TM, Tutomesh

tissue is believed to wrap the prosthesis by granting the right position; unfortunately, excessive fibrous encapsulation may form a stiffer and thicker capsule, with following contracture (Singh-Ranger & Mokbel,

2004). The latter determines pain, soft tissue irritation and leads, from aesthetic point of view, an undesirable appearance of the breast to the patient (Administration FaD, 2011). Additional corrective surgery



may be required to remove the fibrous capsule, resulting in amplified costs for the patient and for the healthcare system (Gardani et al., 2017). Clinical and experimental data supported the evidence that the use of APMs for implant-based breast reconstruction associates with a lower incidence of capsular contracture compared with standard reconstruction (Lee & Mun, 2016). APMs likely protect prostheses and therefore reduce potential prostheses-induced tissue foreign body inflammatory reaction (Schmitz et al., 2013). APMs are made of extracellular matrix proteins and represent a useful device to ameliorate migration, adhesion and cellular proliferation (Lee & Mun, 2016). Being capsular contracture mainly based on excessive connective tissue deposition (Spear, Seruya, Clemens, Teitelbaum, & Nahabedian, 2011; Stump et al., 2009), many studies were performed in order to optimize APM-associated prosthetic implantation. We analyzed and compared tissue remodeling after the implantation of two different APMs (BioRipar and Tutomesh) in prosthetic breast reconstruction in rats. Firstly, we documented some differences in tissue remodeling following the implantation of the two APMs alone. We observed a greater number of intra-APM CD31<sup>+</sup> positive vessels in BioRipar group, already starting 3 weeks after implantation. The formation of new vessels is considered positive and indicates a good integration of APM with surrounding tissue likely favoring the production of nonfibrotic dermal tissue (Kalaba et al., 2016). Similarly, the presence of Ki67<sup>+</sup> proliferating cells inside APMs supports the process of neoangiogenesis and the good tissue integration. In addition, Masson's trichrome staining evidenced a different staining pattern between APMs, likely due to their intrinsic characteristics, but importantly revealed the absence of fibrotic tissue accumulation and the appearance of loose connective tissue also after 24 weeks. This finding is also confirmed by  $\alpha$ -SMA immunoreactivity that showed a moderate increase of expression at 3 and 6 weeks after implantation, especially for Tutomesh APM, likely due to its intrinsic characteristics, since no difference between the two APMs was found as concerning residual components derived from the preparation (Bielli et al., 2018). In fact, at 24 weeks,  $\alpha$ -SMA expression stabilized similarly in both APMs, suggesting a physiological capsular tissue accumulation in the early postsurgical period (Kalaba et al., 2016; Ulrich et al., 2012). In fact, the presence of a moderate amount of myofibroblasts is considered positive for a good integration of the prosthesis and is the direct consequence of the physiological healing process, whose inhibition could be even counterproductive (Kalaba et al., 2016; Ulrich et al., 2012). Instead, an excessive amount of proliferating myofibroblasts can be detrimental since it can induce tissue contracture and fibrosis that represent main long-term complications associated to breast reconstruction (Ulrich et al., 2012). Finally, 3 weeks after implantation, a CD3<sup>+</sup> inflammatory infiltrate was observed around both APMs, as previously observed (Brown et al., 2015). Chronic inflammatory process went back over time; however, CD3<sup>+</sup> cell accumulation was more evident in Tutomesh APM implantation at 24 weeks, suggesting a good tissue response in the APM-dermal integration and the evidence of how the APM biological characteristics can influence the process (Brown et al., 2015).

We also investigated APM-driven tissue remodeling occurring after the combined implantation with three different silicone prostheses. Differences observed in tissue integration, comparing BioRipar and Tutomesh alone, were also confirmed in association with the three different silicone miniprostheses. However, the slight variability found among prostheses within APM groups is likely attributable to the intrinsic characteristics of the prostheses themselves. Some works focused on regenerative surgery highlighted the importance of the biological characteristics of the APM on remodeling and regeneration process.<sup>41</sup> Our data indicated that APMs critically influence the integration process and tissue remodeling following their implantation, and support the combined use of prostheses with APMs for a better tissue remodeling around the implant site.

In conclusion, our results suggest that differences in composition and/or structure of AMP likely influence tissue remodeling after their implantation alone or in combination with different prostheses. Therefore, the quality of the materials employed for APM production may influence the clinical outcome in terms of integration, encapsulation, infiltration, and periprosthetic tissue remodeling. Further studies are needed in order to develop a new APM able to optimize tissue integration and to reduce adverse effects as postsurgical periprosthetic fibrosis.

## ACKNOWLEDGMENTS

This work was partially supported by Assut Europe S.p.A. The authors wish to thank Kalina Gentili, Antonio Volpe, and Sabrina Cappelli for their technical assistance.

## CONFLICT OF INTEREST

All authors declare any commercial association that might pose a conflict of interest in connection with the submitted manuscript.

## REFERENCES

- Administration FaD. *Food & Drug Administration, FDA update on the safety of silicone gel-filled breast implants*. Washington, D.C., 2011.
- Italian Association of Medical Oncology (AIOM), *Linee guida AIOM 2018 Neoplasie della mammella*, Milan, 2018.
- Bertozzi, N., Pesce, M., Santi, P., & Raposio, E. (2017). One-stage immediate breast reconstruction: A concise review. *BioMed Research International*, 2017, 6486859.
- Bielli, A., Bernardini, R., Varvaras, D., Rossi, P., Di Blasi, G., Petrella, G., ... Orlandi, A. (2018). Characterization of a new decellularized bovine pericardial biological mesh: Structural and mechanical properties. *Journal of the Mechanical Behavior of Biomedical Materials*, 78, 420–426.
- Bodai, B. I., & Tusso, P. (2015). Breast cancer survivorship: A comprehensive review of long-term medical issues and lifestyle recommendations. *The Permanente Journal*, 19(2), 48–79.
- Brown, B. N., Mani, D., Nolfi, A. L., Liang, R., Abramowitch, S. D., & Moalli, P. A. (2015). Characterization of the host inflammatory response following implantation of prolapse mesh in rhesus macaque. *American Journal of Obstetrics and Gynecology*, 213(5), 668 e1–668 e10.
- Caffee, H. H. (1986). The influence of silicone bleed on capsule contracture. *Annals of Plastic Surgery*, 17(4), 284–287.

- Chang, I. Y., Hargreaves, W., Segara, D., & Moisidis, E. (2013). Experience in dermomyofascial pouch coverage of immediate implants following skin sparing reduction mastectomy. *ANZ Journal of Surgery*, 83(3), 135–138.
- Darzi, S., Urbankova, I., Su, K., White, J., Lo, C., Alexander, D., ... Deprest, J. (2016). Tissue response to collagen containing polypropylene meshes in an ovine vaginal repair model. *Acta Biomaterialia*, 39, 114–123.
- DellaCroce, F. J., & Wolfe, E. T. (2013). Breast reconstruction. *The Surgical Clinics of North America*, 93(2), 445–454.
- DiEgidio, P., Friedman, H. I., Gourdie, R. G., Riley, A. E., Yost, M. J., & Goodwin, R. L. (2014). Biomedical implant capsule formation: Lessons learned and the road ahead. *Annals of Plastic Surgery*, 73(4), 451–460.
- . (2013). Italian cancer figures, report 2013: Multiple tumours. *Epidemiologia e Prevenzione*, 37(4–5 Suppl. 1), 1–152.
- Ferlay, J., Soerjomataram, I., Dikshit, R., Eser, S., Mathers, C., Rebelo, M., ... Bray, F. (2015). Cancer incidence and mortality worldwide: sources, methods and major patterns in GLOBOCAN 2012. *International Journal of Cancer*.
- Gardani, M., Bertozzi, N., Grieco, M. P., Pesce, M., Simonacci, F., Santi, P., & Raposio, E. (2017). Breast reconstruction with anatomical implants: A review of indications and techniques based on current literature. *Annals of Medicine and Surgery*, 21, 96–104.
- Gubitosi, A., Docimo, G., Parmeggiani, D., Pirozzi, R., Vitiello, C., Schettino, P., ... Docimo, L. (2014). Acellular bovine pericardium dermal matrix in immediate breast reconstruction after skin sparing mastectomy. *International Journal of Surgery*, 12(Suppl. 1), S205–S208.
- Headon, H., Kasem, A., & Mokbel, K. (2015). Capsular contracture after breast augmentation: An update for clinical practice. *Archives of Plastic Surgery*, 42(5), 532–543.
- Kalaba, S., Gerhard, E., Winder, J. S., Pauli, E. M., Haluck, R. S., & Yang, J. (2016). Design strategies and applications of biomaterials and devices for hernia repair. *Bioactive Materials*, 1(1), 2–17.
- Kocan, S., & Gursoy, A. (2016). Body image of women with breast cancer after mastectomy: A qualitative research. *Journal of Breast Health*, 12(4), 145–150.
- Lee, K. T., & Mun, G. H. (2016). Updated evidence of acellular dermal matrix use for implant-based breast reconstruction: A meta-analysis. *Annals of Surgical Oncology*, 23(2), 600–610.
- Maxwell, G. P., & Gabriel, A. (2017). Breast implant design. *Gland Surgery*, 6(2), 148–153.
- Mendes, F. H., Viterbo, F., & DeLucca, L. (2008). The influence of external ultrasound on the histologic architecture of the organic capsule around smooth silicone implants: Experimental study in rats. *Aesthetic Plastic Surgery*, 32(3), 442–450.
- Ng, R., Pond, G. R., Tang, P. A., MacIntosh, P. W., Siu, L. L., & Chen, E. X. (2008). Correlation of changes between 2-year disease-free survival and 5-year overall survival in adjuvant breast cancer trials from 1966 to 2006. *Annals of Oncology*, 19(3), 481–486.
- Orlandi, A., Ciucci, A., Ferlosio, A., Pellegrino, A., Chiariello, L., & Spagnoli, L. G. (2005). Increased expression and activity of matrix metalloproteinases characterize embolic cardiac myxomas. *The American Journal of Pathology*, 166(6), 1619–1628.
- Orlandi, A., Francesconi, A., Cochia, D., Corsini, A., & Spagnoli, L. G. (2001). Phenotypic heterogeneity influences apoptotic susceptibility to retinoic acid and cis-platinum of rat arterial smooth muscle cells in vitro: Implications for the evolution of experimental intimal thickening. *Arteriosclerosis, Thrombosis, and Vascular Biology*, 21(7), 1118–1123.
- Orlandi, A., Francesconi, A., Marcellini, M., Ferlosio, A., & Spagnoli, L. G. (2004). Role of ageing and coronary atherosclerosis in the development of cardiac fibrosis in the rabbit. *Cardiovascular Research*, 64(3), 544–552.
- Racano, C., Fania, P. L., Motta, G. B., Belloni, C., Lazzarini, E., Isoardi, R., ... Ragni, L. (2002). Immediate and delayed two-stage post-mastectomy breast reconstruction with implants. Our experience of general surgeons. *Minerva Chirurgica*, 57(2), 135–149.
- Roostaeian, J., Sanchez, I., Vardanian, A., Herrera, F., Galanis, C., Da Lio, A., ... Crisera, C. A. (2012). Comparison of immediate implant placement versus the staged tissue expander technique in breast reconstruction. *Plastic and Reconstructive Surgery*, 129(6), 909e–918e.
- Sabino, J., Lucas, D. J., Shriver, C. D., Vertrees, A. E., Valerio, I. L., & Singh, D. P. (2016). NSQIP analysis: Increased immediate reconstruction in the treatment of breast cancer. *The American Surgeon*, 82(6), 540–545.
- Schmitz, M., Bertram, M., Kneser, U., Keller, A. K., & Horch, R. E. (2013). Experimental total wrapping of breast implants with acellular dermal matrix: A preventive tool against capsular contracture in breast surgery? *Journal of Plastic, Reconstructive & Aesthetic Surgery*, 66(10), 1382–1389.
- Scioli, M. G., Stasi, M. A., Passeri, D., Doldo, E., Costanza, G., Camerini, R., ... Orlandi, A. (2014). Propionyl-L-Carnitine is efficacious in ulcerative colitis through its action on the immune function and microvasculature. *Clinical and Translational Gastroenterology*, 5, e55.
- Seyhan, H., Kopp, J., Beier, J. P., Vogel, M., Akkermann, O., Kneser, U., ... Horch, R. E. (2011). Smooth and textured silicone surfaces of modified gel mammary prostheses cause a different impact on fibroproliferative properties of dermal fibroblasts. *Journal of Plastic, Reconstructive & Aesthetic Surgery*, 64(3), e60–e66.
- Silva, M. M., Modolin, M., Faintuch, J., Yamaguchi, C. M., Zandona, C. B., Cintra, W., Jr., ... Ferreira, M. C. (2011). Systemic inflammatory reaction after silicone breast implant. *Aesthetic Plastic Surgery*, 35(5), 789–794.
- Singh-Ranger, G., & Mokbel, K. (2004). Capsular contraction following immediate reconstructive surgery for breast cancer—An association with methylene blue dye. *International Seminars in Surgical Oncology*, 1(1), 3.
- Somogyi, R. B., Ziolkowski, N., Osman, F., Ginty, A., & Brown, M. (2018). Breast reconstruction: Updated overview for primary care physicians. *Canadian Family Physician*, 64(6), 424–432.
- Spear, S. L., Seruya, M., Clemens, M. W., Teitelbaum, S., & Nahabedian, M. Y. (2011). Acellular dermal matrix for the treatment and prevention of implant-associated breast deformities. *Plastic and Reconstructive Surgery*, 127(3), 1047–1058.
- Stasi, R. (2010). An overview of pharmacotherapy for anti-neutrophil cytoplasmic antibody-associated vasculitis. *Drugs Today (Barc)*, 46(12), 919–928.
- Stump, A., Holton, L. H., 3rd, Connor, J., Harper, J. R., Slezak, S., & Silverman, R. P. (2009). The use of acellular dermal matrix to prevent capsule formation around implants in a primate model. *Plastic and Reconstructive Surgery*, 124(1), 82–91.
- Ulrich, D., Edwards, S. L., White, J. F., Supit, T., Ramshaw, J. A., Lo, C., ... Gargett, C. E. (2012). A preclinical evaluation of alternative synthetic biomaterials for fascial defect repair using a rat abdominal hernia model. *PLoS One*, 7(11), e50044.
- Yamashita, M., Ogawa, T., Zhang, X., Hanamura, N., Kashikura, Y., Takamura, M., ... Shiraishi, T. (2012). Role of stromal myofibroblasts in invasive breast cancer: Stromal expression of alpha-smooth muscle actin correlates with worse clinical outcome. *Breast Cancer*, 19(2), 170–176.
- Zhu, L. M., Schuster, P., & Klinge, U. (2015). Mesh implants: An overview of crucial mesh parameters. *World Journal of Gastrointestinal Surgery*, 7(10), 226–236.

## SUPPORTING INFORMATION

Additional supporting information may be found online in the Supporting Information section at the end of this article.

**How to cite this article:** Bernardini R, Varvas D, D'Amico F, et al. Biological acellular pericardial mesh regulated tissue integration and remodeling in a rat model of breast prosthetic implantation. *J Biomed Mater Res*. 2019;1–14. <https://doi.org/10.1002/jbm.b.34413>